Proceedings of ASME Turbo Expo 2011
GT2011
June 6-10, 2011, Vancouver, British Columbia, Canada

GT2011-45142

PERFORMANCE OF A SHOWERHEAD AND SHAPED HOLE FILM COOLED VANE AT HIGH FREESTREAM TURBULENCE AND TRANSONIC CONDITIONS

A. Newman, S. Xue, W. Ng
Mechanical Engineering
Virginia Polytechnic Institute and State University
Blacksburg, VA, USA

H.K. Moon and L. Zhang
Solar Turbines Incorporated
San Diego, CA, USA

ABSTRACT

An experimental study was performed to measure surface Nusselt number and film cooling effectiveness on a film cooled first stage nozzle guide vane using a transient thin film gauge (TFG) technique. The information presented attempts to further characterize the performance of shaped hole film cooling by taking measurements on a row of shaped holes downstream of leading edge showerhead injection on both the pressure and suction surfaces (hereafter PS and SS) of a 1st stage NGV. Tests were performed at engine representative Mach and Reynolds numbers and high inlet turbulence intensity and large length scale at the Virginia Tech Transonic Cascade facility. Three exit Mach/Reynolds number conditions were tested: 1.0/1,400,000; 0.85/1,150,000; and 0.60/850,000 where Reynolds number is based on exit conditions and vane chord. At Mach/Reynolds numbers of 1.0/1,450,000 and 0.85/1,150,000 three blowing ratio conditions were tested: BR = 1.0, 1.5, and 2.0. At a Mach/Reynolds number of 0.60/850,000, two blowing ratio conditions were tested: BR = 1.5 and 2.0. All tests were performed at inlet turbulence intensity of 12% and length scale normalized by the cascade pitch of 0.28. Film cooling effectiveness and heat transfer results compared well with previously published data, showing a marked effectiveness improvement (up to 2.5x) over the showerhead only NGV and agreement with published showerhead-shaped hole data. Net heat flux reduction was shown to increase substantially (average 2.6x) with the addition of shaped holes, with an increase (average 1.6x) in required coolant mass flow. Boundary layer transition location was shown to be within a consistent region on the suction side regardless of blowing ratio and exit Mach number.

INTRODUCTION

As gas turbine manufacturers ever strive for higher efficiency and increased output from their products, turbine inlet temperatures have been increasing as a way to meet this end. The industry is already to a point where turbine inlet temperatures have reached greater values than blade and vane materials can withstand. In response to this problem, techniques such as complex internal and film cooling schemes and thermal barrier coatings have been employed to help increase engine component life and performance. This study attempts to further characterize the performance of shaped hole film cooling by taking measurements on a row of shaped holes downstream of leading edge showerhead injection on both the pressure and suction surfaces (hereafter PS and SS) of a 1st stage NGV. Data is not readily available in literature for the performance of a single row of shaped holes with showerhead interaction at high freestream turbulence intensity, large length scale, and engine-realistic Mach and Reynolds numbers.

The freestream turbulence level has a substantial effect on vane surface heat transfer. Goldstein *et al.* [1] and Koutmos and McGuirk [2] determined the turbulence intensity of 15% to 30% at the combustor exit, using can-type model with swirlers and dilution jets. Considering the equivalent turbulent kinetic energy in a transonic cascade test, the turbulence intensity level above 10% at inlet is enough to simulate the engine condition. Inlet freestream turbulence greater than 10% is usually employed by researchers in the cascade tunnel tests. For example Reiss and Bölcs [3] did their tests at Tu=10%; Ames [4] operated the experiment at Tu=12%; Guo *et al.* [5] ran their tests with Tu=13%, to list a few. The highest levels seen in the literature is about 20%, but those tests are operated at a very low speed, such as Cutbirth and Bogard [6] with an inlet velocity of 5.8m/s and Ou *et al.*[7] with an inlet velocity of 10m/s. In this paper all the tests were operated with an inlet freestream turbulence intensity level of 12%, and at transonic exit condition.

Initial research performed by Goldstein *et al.* [8] demonstrated the potential of shaped hole film cooling above and beyond that of cylindrical holes in simplified-geometry flat plate experiments. Since that time, many others have explored the effects of injection angle, row spacing, row interaction, hole shaping, and many other parameters that have a bearing on film cooling performance. Many have looked into the effect of hole shaping by way of low speed flat plate studies such as Schmidt *et al.* [9], Gritsch *et al.* [10], and Yu *et al.* [11]. Studies such as these explore different expansion angles in the span and streamwise directions, often comparing back to rows of cylindrical holes to emphasize shaped hole performance benefits. Studies such as Bell *et al.*[12], Dittmar *et al.* [13], and Yuen *et al.* [14] have expanded on Goldstein *et al.* [8] to include comparisons of single and multiple rows of fan shaped holes to multiple rows of cylindrical holes with compound injection and rows of slot-type holes. As it has proved so beneficial to cylindrical holes, compound injection for shaped holes has also been a topic of interest in the previous three studies as well. Many other design factors have been explored by way of low speed flat or curved plate experiments such as: hole trenching and tabs (Lu *et al.* [15], Dhungel *et al.* [16]), shaped hole channel and surface flowfields (Wittig *et al.* [17], Thole *et al.* [18], Saumweber and Schulz [19]), effect of mainstream turbulence (Saumweber *et al.* [20]) and row spacing (Saumweber and Schulz [19]) to name a few.

Shaped hole research has also been performed on NGVs in low-speed linear cascades. These studies tend to approximate engine Reynolds numbers by way of scaling, however they do not accurately represent engine-realistic Mach number. Colban *et al.* [21] performed heat transfer and film effectiveness measurements in a low-speed cascade using a steady state IR technique. This study looked at the effect of upstream blowing, and showed that the presence of upstream blowing reduced the incidence of jet-liftoff at higher blowing ratios. Colban *et al.* [22] also performed a comparison of experimental shaped hole data with CFD using different turbulence models, showing that the RNG k-ε turbulence model better predicted effectiveness levels. Chappell *et al.* [23] performed a comparison of hole types and angles in a low speed cascade, concluding that compound angle had more effect on film cooling performance than hole shape.

In addition to low speed cascade studies, others have performed curved or flat plate studies at transonic Mach numbers to evaluate shaped hole performance. Wittig *et al.* [17] explored internal and external flowfield on a transonic flat plate rig. Furukawa *et al.* [24] explored the effects of hole shape and angle on a suction side airfoil model finding that fan shaped holes at compound angles show a significant effectiveness benefit over shaped holes and cylindrical holes without compound injection.

There are many studies exploring fan shaped holes at low Mach numbers and/or with simplified geometry, however there are comparatively fewer with engine representative Mach numbers. Fewer still are fan shaped hole cascade studies performed on vanes at high turbulence and engine representative Mach and Reynolds numbers. Zhang and Pudupatty [25] and Zhang *et al.* [26] look at PS and SS film effectiveness (respectively) on a first stage NGV with showerhead and shaped hole film cooling. Tests were performed at transonic exit Mach numbers (0.74 and 0.61) and high inlet turbulence intensity (12%). Their findings in both cases were that upstream injection reduced the tendency of jet liftoff at high blowing ratios, and that little effectiveness benefit was seen from shaped holes at blowing ratios above 2. Zhang and Pudupatty [25] also found that at higher blowing ratios, showerhead injection augmented the effectiveness of downstream film cooling rows on the PS. Schnieder *et al.* [27] performed a study to investigate the effects of showerhead and PS row interaction at high inlet turbulence and high exit Mach number. Their findings indicated that the increased turbulence created by showerhead injection caused more rapid film diffusion of downstream rows of shaped holes. Other studies such as Thurman *et al.* [28] have looked at heat transfer due to shaped hole film cooling, showing local increases in injection regions.

In addition to linear cascade studies others have explored rows of shaped holes in annular cascades. Guo *et al.* [29] looked at the effect of using foreign gasses for coolant to achieve engine-representative density ratios in a transonic annular cascade. Sargison *et al.* [30] compared a converging-slot hole geometry to fan shape holes in the same facility as Guo *et al.* [29].

This paper will present the results of heat transfer and effectiveness measurements on a film cooled NGV with five rows of showerhead film cooling and one row of fan shaped holes on both the pressure and suction sides. These results are measured at three engine-representative exit Mach/Reynolds numbers and high inlet turbulence. The main objectives of this paper are to: investigate the effect of Mach number and blowing ratio on showerhead and downstream shaped hole film cooling, to compare showerhead only with combined showerhead and shaped hole film cooling at multiple blowing ratios and Mach numbers, and to perform a NHFR comparison to illustrate the overall effect of adding shape hole cooling rows.

EXPERIMENTAL FACILITY AND INSTRUMENTATION

Tests were performed in the Virginia Tech Transonic Cascade tunnel. This is a transient blowdown facility, a schematic of which can be seen in Figure 1. The facility is also equipped with a heat exchanger capable of heating the mainstream flow to 150˚C (423˚K) for heat transfer testing. For heat transfer testing, there is a 10-15 second window of steady tunnel response in which data is taken. Inlet turbulence is generated directly upstream of the test section by way of a passive mesh grid. The turbulence grid and its relation to the cascade can be seen in Figure 2 for these experiments this grid generates a turbulence intensity of 12% and turbulence length scale nondimensionalized by the cascade pitch of 0.28. This facility has been used by Reagle *et al.* [31], Bolchoz *et al.* [32], and Nasir *et al.* [33], [34] for vane and blade aerodynamic and heat transfer testing.

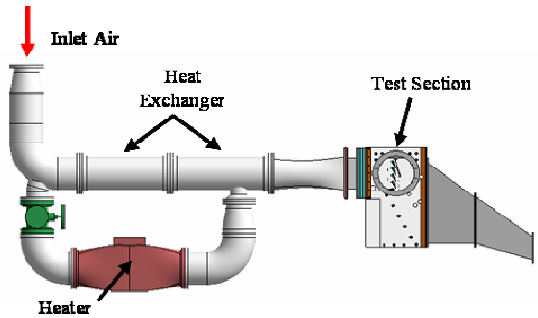

Figure 1: Virginia Tech Transonic Cascade facility

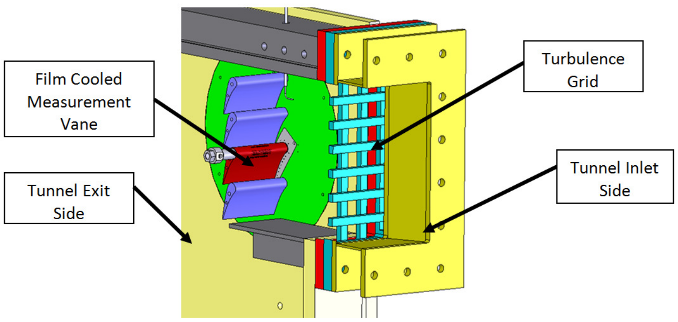

Figure 2: Close-up of vane test section

The vane profile is that of a first stage NGV provide by Solar Turbines, Inc., and is scaled 1.5x to match engine Reynolds numbers. Detailed aerodynamic performance of this vane cascade has been previously published by Nasir *et al.* [33]. Details on the vane geometry can be found in Table 1.

Table 1: Showerhead-shaped hole vane parameters

Chord	C	91.19 mm
Pitch	P	83.06 mm
Span	-	152.40 mm
Film-Cooled Span	-	59.18 mm
Inlet Angle	-	0 degree
Exit Angle	-	73.5 degree
Coolant Metering Hole Diameter	d	0.79 mm

Heat transfer measurements are taken on the center vane in the cascade. This vane is made of Corning Macor® machineable glass-ceramic. Macor® is chosen for its relatively low thermal diffusivity and conductivity, allowing for the use of a 1-D semi-infinite assumption in data reduction. The center vane has a total of seven rows of film cooling holes: Five rows of showerhead cooling on the LE, one row of shaped holes on the SS and one row of shaped holes on the PS.

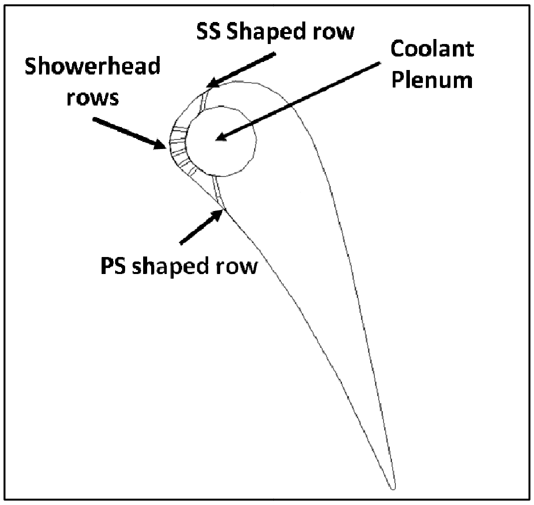

Figure 3: Showerhead-shaped hole vane profile

The film cooled vane is instrumented with 25 thin-film type heat flux sensors (TFGs). The gages used in this study are designed similar to that of Doorly and Oldfield [35] and are manufactured by AFRL using the method described in Joe [37]. The gages are applied to the measurement vane at 45% span, and are oriented such that the platinum sensing element is along a shaped hole centerline. Ten gages are instrumented on the PS of the vane, and 15 are instrumented on the SS. Before assembling the wind tunnel, the gages are placed in a thermocouple incubator for calibration.

DATA REDUCTION

A finite difference code described by Nasir *et al.* [34] and developed by Cress [38] is used to calculate heat flux, *q"*. This finite difference code solves the 1-D transient conduction equation for *q"* (eq. 1) based on the time response of the vane surface temperature and the thermal properties of the vane material.

$$\frac{\partial^2 T}{\partial x^2} = \frac{1}{\alpha}\frac{\partial T}{\partial t} \tag{1}$$

Heat transfer coefficient and film cooling effectiveness are derived using a linear regression method developed by Popp *et al.* [39]. This method starts with the convective heat transfer equation

$$q" = h(T_{aw} - T_w) \tag{2}$$

and the equation for film cooling effectiveness (non-dimensionalized adiabatic wall temperature).

$$\eta = \frac{T_{aw} - T_r}{T_c - T_r} \tag{3}$$

Where T_c is the coolant total temperature in the plenum. Equations 2 and 3 are then combined to yield an equation expressing heat transfer coefficient and film cooling effectiveness in the form y = mx + b.

$$\frac{q''}{T_r - T_c} = h\left(\frac{T_r - T_w}{T_r - T_c}\right) - h \cdot \eta \qquad (4)$$

For this study heat transfer coefficient will be nondimensionalized by way of Nusselt number as defined in equation 5.

$$Nu = \frac{h \cdot C}{k_a} \qquad (5)$$

To reduce experimental uncertainty a double-regression method was used, whereby two sets of data are used to perform the linear regression. For this technique two runs are performed at identical flow conditions but with different coolant temperatures. This technique reduces uncertainty by increasing the number of data points used for regression and adding points closer to the x-axis, reducing the distance the line fit is extrapolated to calculate effectiveness. Figure 4 shows the line fit for a double regression run.

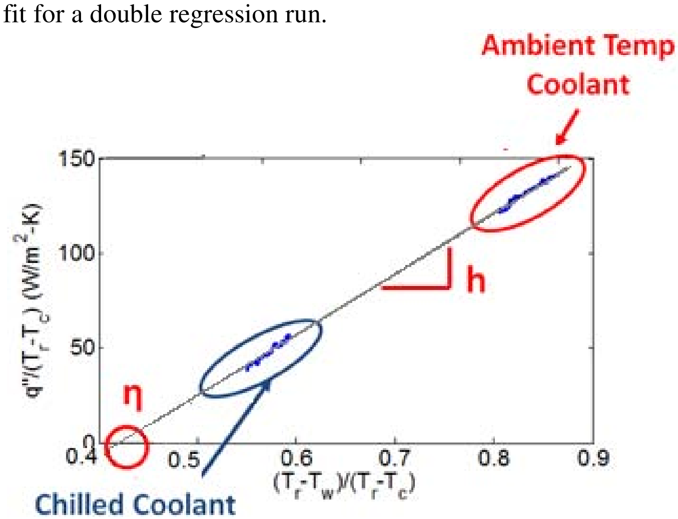

Figure 4: Double regression line fit

When using chilled coolant, the coolant to mainstream density ratio changes from the room temperature case. All room temperature runs were completed at a density ratio of 1.45 and all chilled coolant runs were completed at a density ratio of 1.85. Ekkad *et al.* [40] have shown that increasing coolant density ratio can have effects on film effectiveness and Nusselt number distributions for BR<1.0. However, in the present study, all cases considered are at BR>1.0, and hence film effectiveness distributions should only be effected slightly by the difference in density ratios.

Uncertainty is calculated based on errors present in measured data which are propagated first through the finite-difference calculation of q'' then through the linear regression of heat transfer coefficient and film effectiveness. To calculate overall uncertainty, errors present in the x and y-axis of the linear regression line-fit are quantified. Error in heat flux is calculated using Moffat's [41] perturbation method due to the finite difference code used to calculate this quantity. Brown and Coleman's [42] linear regression analysis is then used to calculate the uncertainty of heat transfer coefficient and film effectiveness based on the x and y-axis uncertainties.

This analysis showed an average uncertainty in heat transfer coefficient of ± 7% and an average uncertainty in film effectiveness of ± 0.05. In addition to this analysis, tunnel repeatability was established for each Mach number case. More details on the experiment setup, data reduction and uncertainty analysis can be found in Newman's thesis [43].

SURFACE MEASUREMENT RESULTS

Measurement results will first be compared with past studies performed by this group on a showerhead-only film cooled NGV using the same transient TFG technique. Results will also be compared to other available literature with similar Mach/Reynolds numbers, film cooling configurations, and turbulence levels. Following the comparison, most of the test conditions listed in table 2 will be presented, and the comprehensive result is given in Newman's thesis [43]. Results will be presented in terms of Nusselt number distributions and film cooling effectiveness distributions.

Table 2: Test matrix of surface measurements

Film Cooled Test Matrix			
Ma	**Re**	**Tu**	**BR, MFR %**
0.60	850,000	12%	1.5, 1.04
			2.0 , 1.15
0.85	1,150,000		1.0, 0.85
			1.5, 1.04
			2.0 , 1.15
1.00	1,400,000		1.0, 0.85
			1.5, 1.04
			2.0 , 1.15

Three blowing/mass flow ratios were tested at two exit Mach numbers (M_{ex} = 1.0 and 0.85) with only two blowing/mass flow ratios tested at the low exit Mach number case of M_{ex} = 0.60. The low coolant flow rates required for BR = 1.0 at the low exit Mach number case of M_{ex} = 0.60 exceeded the lower physical limitations of the film cooling loop, resulting in non-repeatability. Results will be reported in terms of exit Mach number and blowing ratio, where blowing ratio is defined as the ratio of coolant density times velocity to freestream density times velocity. Equation 6 shows this relationship.

$$BR = \frac{\rho_c U_c}{\rho_\infty U_\infty} \qquad (6)$$

Mass flow ratio is the relationship of total coolant mass flow for all film cooling rows to passage mass flow as defined below in equation 7.

$$MFR\% = \frac{\dot{m}_c}{\dot{m}_p} \tag{7}$$

All seven rows of film cooling holes (five LE showerhead, one SS shaped, and one PS shaped) are fed from a common plenum. The local blowing ratios of showerhead, SS shaped holes, and PS shaped holes were determined by the plenum total pressure and the surface static pressures at exit of each cooling row respectively. As a result of local velocity difference the local blowing ratios differ remarkably between SS shaped holes and PS shaped holes. Table 3 shows the relationship between showerhead blowing ratio and shaped hole blowing ratio for each of the three blowing ratio cases tested. It can be observed that when showerhead blowing ratio changed from 1.0 to 2.0 the PS shaped hole blowing ratio changed from 1.7 to 3.0 (76% increase), but SS shaped hole blowing ratio only changed from 1.1 to 1.4 (27% increase). The uneven changing of PS and SS blowing ratio caused different trend of cooling effectiveness and Nusselt number on PS and SS, and this will be discussed later in the result section.

Table 3: Relationship between showerhead and shaped hole BR

BR Showerhead	BR PS Shaped	BR SS Shaped
2.0	3.0	1.4
1.5	2.2	1.2
1.0	1.7	1.1

This paper will compare data from the present study with data from Nasir *et al.* [34], a study performed in the same facility but with showerhead film cooling only. In order to compare film effectiveness and Nusselt number between the two film cooling designs, the increase in coolant mass flow required by the addition of two shaped hole rows to the existing showerhead film cooled vane must be quantified. To perform this analysis, total coolant mass flow rates for the showerhead and shaped hole vane from the present study at M_{ex} = 0.85, BR = 2.0 were averaged over multiple runs. This value was then divided by the total coolant mass flow rate for the showerhead only vane (Nasir *et al.* [34] at M_{ex} = 0.80, BR = 2.0) averaged over multiple runs. The result of this simple calculation showed that the addition of shaped holes resulted in an average 1.6x increase in total coolant usage over the showerhead only film cooled vane presented in Nasir *et al.* [34].

Literature Comparisons

Figures 5 and 6 show comparisons of the present study with Zhang *et al.* [25], [26] and Schnieder *et al.* [27]. Zhang et al [25], [26] were performed on an NGV of the same profile with similar hole shapes, but different injection locations. Schnieder *et al.* [27] is a showerhead-shaped hole interaction study performed on the PS only. Both studies report only film cooling effectiveness and do not measure Nusselt number.

Results in this section will be plotted for the near hole region only, the entire blade surface will not be compared. Figure 5 is a pressure side results comparison where the origin of the axis is the shaped holes injection location and streamwise distance on the PS increases to the right of the plot. Figure 6 is a comparison of SS effectiveness where the origin of axis is the shaped hole injection location, and streamwise distance down the SS increases to the right of the plot.

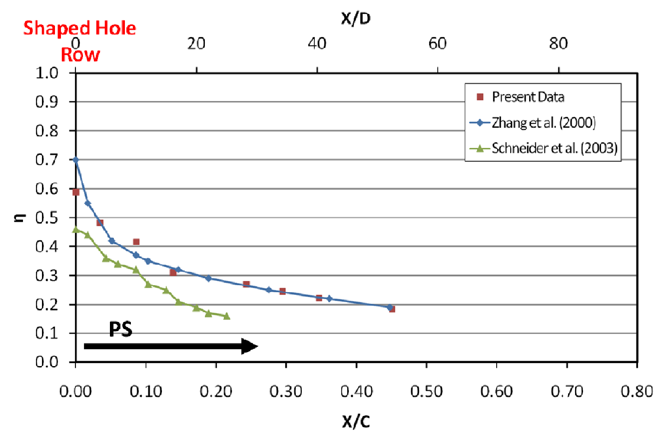

Figure 5: PS effectiveness literature comparison

The present study shows very good agreement with Zhang *et al.* [25] on the PS of the vane (Fig. 5). Slight differences may be attributed to changes in injection location, but overall it shows a good match in trend and level. The comparison between Schnieder *et al.* [27] is not as close as the comparison with Zhang *et al.* [25], however they still compare favorably. One of the main conclusions of Schnieder *et al.* [27] was that upstream showerhead injection increased local turbulence resulting in faster shaped hole diffusion and lower effectiveness values. This may also be a function of row spacing. Both the present study and Zhang *et al.* [25] had significantly larger spacing between showerhead injection and the first row of shaped holes. This increased spacing may provide room for local turbulence due to showerhead injection to dissipate, resulting in less of a diffusion effect on the shaped hole rows and higher levels of effectiveness than reported by Schnieder *et al.* [27].

On the SS, the present study again shows very good agreement with Zhang *et al.* [26] (Fig. 6). Slight differences in trend and level may be explained by some of the differences in the studies. First, Zhang *et al.* [26] ran their tests at exit Mach numbers lower than the present study, possibly accounting for slightly lower effectiveness values in the region 10<X/D<40. Second, Zhang *et al.* [26] had multiple rows of suction side injection at considerably different locations. The sharp decrease in effectiveness shown at 5<X/D<10 may be a result of their first row of shaped holes being placed closer to the throat. This row of holes may be experiencing transition sooner than the present study, resulting in faster diffusion and effectiveness decay. The data plotted from Zhang *et al.* [26] in figure 6 is for the first row of shaped hole cooling on the suction side. In summary, the present data compares reasonably well with published data from similar studies.

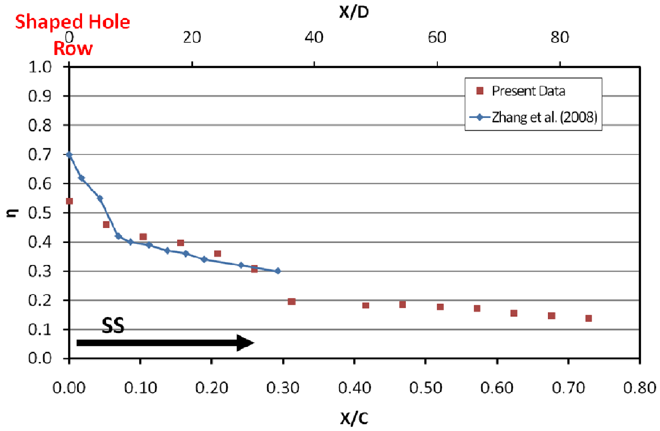

Figure 6: SS effectiveness literature comparison

Laminar and Turbulent Flat Plate Correlation

Figures 7 and 8 show experimental Stanton number distributions from the present study compared with laminar and turbulent flat plate Stanton number predictions. This comparison is useful for gaining fundamental insight into how the boundary layer is behaving on the surface of the vane. It also serves to show whether or not the data falls within an acceptable range of values. For this comparison, the analytical solutions for laminar and turbulent flat plate Nusselt number as presented in Incorpera and De Witt [44] are used. Equation 8 is the laminar boundary layer equation and equation 9 is the turbulent boundary layer equation.

$$Nu_x = 0.332 Re_x^{1/2} Pr^{1/3} \qquad (8)$$

$$Nu_x = 0.0296 Re_x^{4/5} Pr^{1/3} \qquad (9)$$

Both of these equations use vane surface distance from the leading edge as the characteristic length parameter in the calculation of Nusselt number and Reynolds number. Results are then converted from Nusselt number to Stanton number using equations 10 and 11 below.

$$h_x = \frac{Nu_x \cdot k_a}{x} \qquad (10)$$

$$St = \frac{h_x}{\rho_x U_x C_{p,\infty}} \qquad (11)$$

Figures 7 and 8 show experimental data at M_{ex} = 0.85 and BR = 2.0 normalized in terms of Stanton number. Also plotted are the analytical Stanton number solutions for flat plate laminar and turbulent boundary layer cases calculated using equations 8 and 9.

Figure 7 shows the comparison of PS data to the flat plate correlations. Experimental data shows a fairly good match with the turbulent boundary layer solution for most of the PS. The level of the data suggests that the boundary layer is turbulent for the entire length of the PS, and may be a result of high inlet turbulence intensity (12%). This type of heat transfer augmentation resulting from high turbulence intensity has also been shown experimentally by Blair [45]. The presence of film cooling may also be effecting the experimental Stanton number distribution, creating the large heat transfer augmentation (1.8x the turbulent flat plate solution) seen at lower Reynolds numbers which correspond to the near shaped hole region.

Figure 8 shows the comparison on the SS, and boundary layer transition is clearly evident on the plot. Most of the data falls between the laminar and turbulent correlation lines up to the transition point, where data shifts to more closely follow the turbulent correlation. The effect of heat transfer augmentation due to film cooling and inlet turbulence can also be seen before transition in the level and slope difference between the correlations and experimental data.

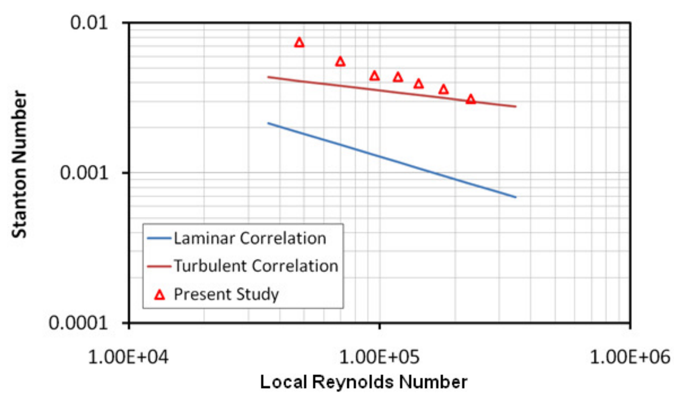

Figure 7: PS M_{ex} = 0.85 BR = 2.0 data compared with flat plate correlations

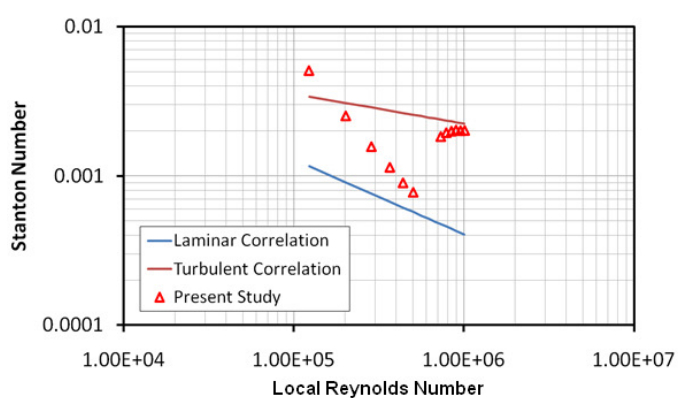

Figure 8: SS M_{ex} = 0.85 BR = 2.0 data compared with flat plate correlations

Comparison with Showerhead-Only Vane

Figure 9 shows a film cooling effectiveness comparison at M_{ex} = 0.85, BR = 2.0 of the data from the present study with that of Nasir *et al.* [34]. Nasir *et al.* [34] presents data taken on a vane of the same profile as the present study with only LE showerhead film cooling.

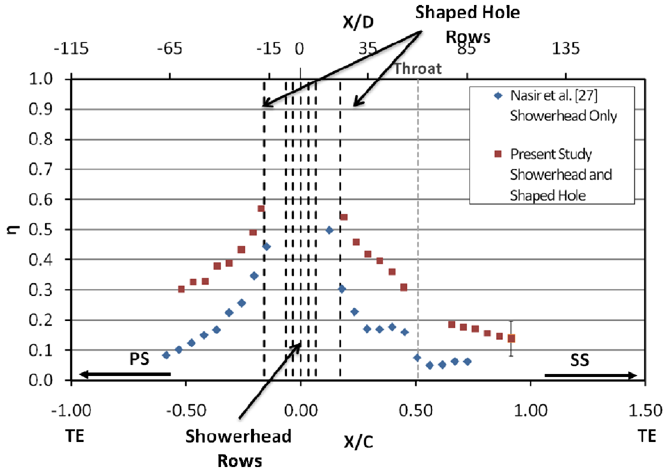

Figure 9: Film cooling effectiveness comparison at M_{ex} = 0.85, BR = 2.0

The comparison shows that the addition of shaped hole rows on the PS and SS has increased film effectiveness across the board. Shaped holes show a 2-2.5x improvement in effectiveness over showerhead only film cooling across the measurement range with only a 1.6x increase in coolant usage. It should also be noted that the shaped holes hold higher effectiveness values farther downstream than the showerhead rows. This is to be expected with shaped holes as they have been shown to diffuse less rapidly with streamwise distance than cylindrical hole cooling. One particular area of interest for both studies has been 0.3<X/C<0.50. In this region the showerhead only data shows an effectiveness plateau, while the showerhead and shaped hole vane shows a sharp effectiveness decrease. Nasir *et al.* [34] attributed the effectiveness plateau to high values of acceleration in this region. High acceleration could have a laminarizing effect on the boundary layer, resulting in delayed film diffusion and the effectiveness plateau seen in the figure. This plateau then decays around the throat where the boundary layer transitions to full turbulence. Based on the present findings, the high acceleration in the region does not appear to have as significant an effect on shaped hole injection.

Figure 10 shows a comparison of Nusselt number between data from Nasir *et al.* [34] at M_{ex} = 0.76, BR = 2.0 and the present study at M_{ex} = 0.85 and BR = 2.0. The first noticeable feature of this plot is considerably higher heat transfer in the near shaped hole region. This may be due to increased mixing and local turbulence directly at the injection site. However, on the SS downstream of injection, Nusselt number values drop below that of the showerhead case, showing what appears to be delayed transition as compared to the showerhead-only data. The exact reason of this occurring is not yet known, further research is required to explore the cause. One of the possible explanations for this trend is that the shaped hole injection added kinetic energy into the boundary layer, which mitigated the velocity gradient, therefore, reducing the shear stress. It is true especially in the outer layer of the turbulent boundary layer that developed on a convex surface [35]. It was shown by Gillis and Johnston [46] that reduction of turbulent shear stress related to surface heat flux reduction. As a result the shaped hole injection on SS reduced the surface heat flux, and lowered the Nusselt number.

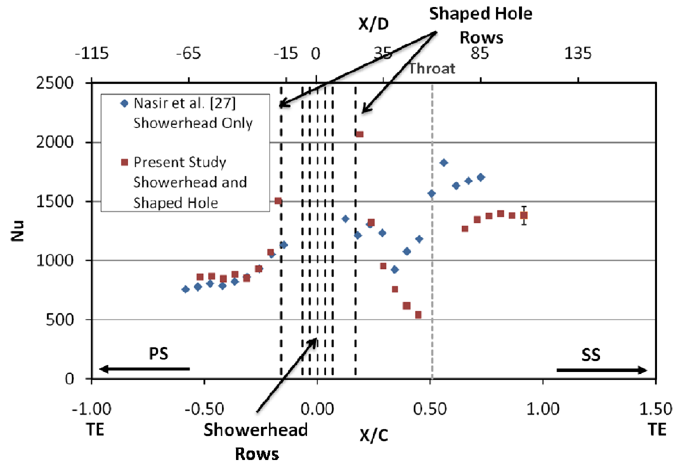

Figure 10: Film cooling Nusselt number comparison, M_{ex} = 0.85, BR = 2.0

Effect of Exit Mach Number on Film Effectiveness

Figure 11 highlights the effect of increasing exit Mach/Reynolds number on film effectiveness distributions at a given blowing ratio of BR=2.0. Generally, increasing the exit Mach number results in increased film effectiveness. This trend has been shown previously in literature by Mehendale and Han [47] for showerhead injection, and by E. Lutum *et al.* [48] on a convex surface for shaped hole injection. In the report, E. Lutum *et al.* suggested the increased freestream Mach number improves the cooling effectiveness by slightly changing the boundary layer thickness and suppressing the boundary layer turbulence production. However, they did not give much detail in their discussion. Besides E. Lutum *et al.*'s analysis [48], another possible explanation could be that by increasing the freestream Mach number, the time for coolant diffusion was reduced as it travels through the same distance on the vane surface, which improves the local cooling performance.

It could also be observed in Figure 11 the effectiveness value of M_{ex} = 1.0 and M_{ex} = 0.85 are very close to each other. That may be because the local Mach number distribution for these two exit Mach number cases are almost identical on both PS and SS before the throat.

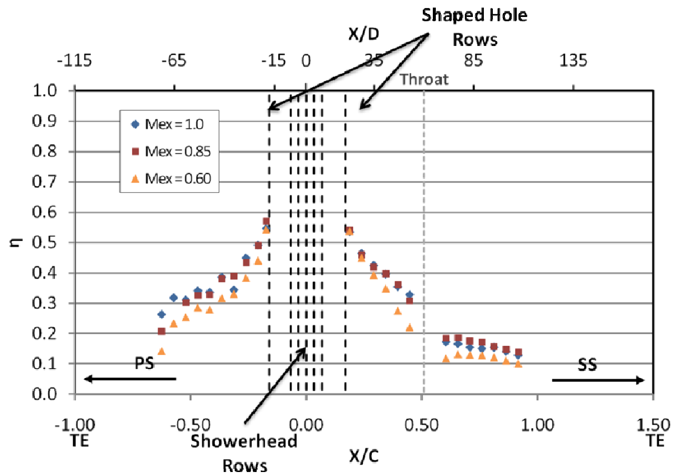

Figure 11: Effect of exit Mach number on film effectiveness distribution, BR = 2.0

Effect of Blowing Ratio on Film Effectiveness

Figures 12 and 13 highlight the effect of increasing blowing ratio on film effectiveness distributions.

In Figure 12 the general trend is that increases in blowing ratio increases film effectiveness. However, as compared with the PS, the effectiveness on SS is less sensitive to the blowing ratio change. This may be due (in part) to the different blowing ratios at the PS and SS shaped hole rows as a result of the vane's single plenum design. As it was shown in Table 3 when the showerhead blowing ration changed from 1.0 to 2.0, the PS blowing ratio increased from 1.7 to 3.0, whereas, the SS blowing ratio only increased from 1.1 to 1.4. Less change of effectiveness on the SS compare to the PS was also observed by Shantanu Mhetras *et al.* [49]. In their test the same plenum was shared by SS and PS cooling holes, and they attribute the minor increase of effectiveness on SS to the smaller increase of SS blowing ratio.

For M_{ex} = 1.0 (Fig. 13), on PS the lower blowing ratio cooling has the same effectiveness as the higher blowing ratio ones, and the SS effectiveness even shows slightly higher effectiveness values at lower blowing ratios. Nasir *et al.* [34] showed this trend at M_{ex} = 1.0 as well, and attributed it to the beginnings of jet liftoff at the higher blowing ratios combined with increased momentum of the freestream resulting in faster film diffusion. However, in the current study the shaped hole injection is not supposed to liftoff with the tested blowing ratio. The reason for this trend is not yet clear at M_{ex} = 1.0, further study is required to determine the cause.

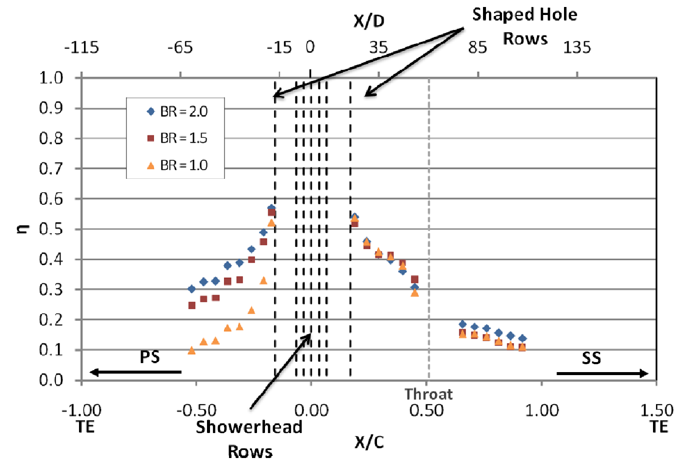

Figure 12: Effect of blowing ratio on film effectiveness, M_{ex} = 0.85

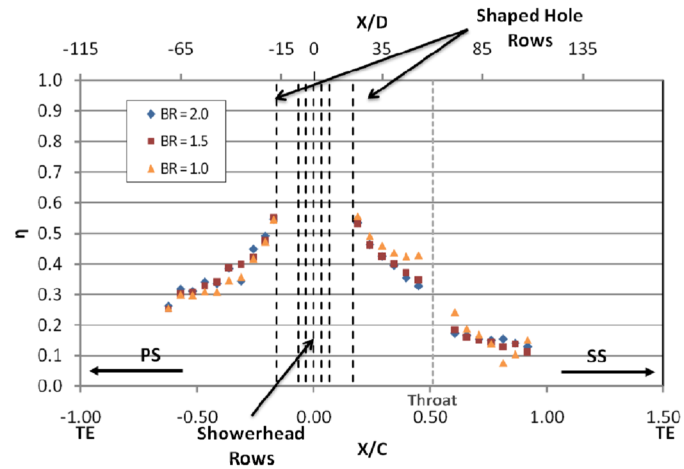

Figure 13: Effect of blowing ratio on film effectiveness, M_{ex} = 1.0

Effect of Exit Mach Number on Nusselt Number

Figure 14 shows the effect of increasing exit Mach number on Nusselt number for the blowing ratio of BR=2.0.

Increasing exit Mach number has the apparent effect of augmenting Nusselt number on both the PS and SS of the measurement vane. A trend of increasing Nusselt number with increasing Mach number has been shown by Nasir *et al.* [34] as well as others such as Reiss and Bölcs [3] and Abuaf *et al.* [50]. The region where transition occurs does not appear to be effected by change in Mach/Reynolds number. It is occurring in approximately the same region just upstream of the throat, and is identified by the sharp jump in Nusselt number seen on the SS. A lack of change in transition region with changing exit Mach number is consistent with the findings of Nasir *et al.* [34] on the showerhead-only vane.

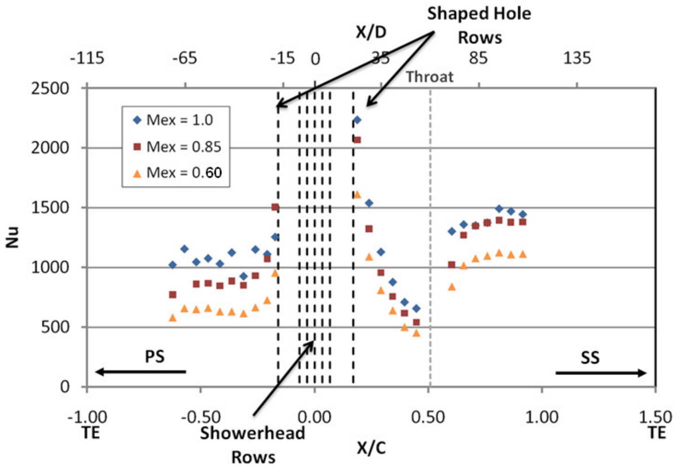

Figure 14: Effect of exit Mach number on Nusselt number distribution, BR = 2.0

Effect of Blowing Ratio on Nusselt Number

Figures 15 and 16 show the effect of blowing ratio on Nusselt number for M_{ex} = 0.85 and M_{ex} = 1.0. In general, as blowing ratio increases, Nusselt number increases on the PS.

For M_{ex} = 0.85 (Fig. 15), The SS also shows little change for all three blowing ratio cases. This may be a result of lower blowing ratio changes from the SS shaped holes due to the single-plenum coolant feed design as mentioned in the discussion of effectiveness results. On the PS, a trend of increasing Nusselt number with increasing blowing ratio is observed. Nusselt number augmentation as a result of higher blowing ratios is generally a result of increased local turbulence due to coolant injection and mixing. This trend has been seen elsewhere in literature such as Arts *et al.* [51] and Ekkad *et al.* [52] to name two. As was the case with varied exit Mach number, the location of boundary layer transition does not appear to change with blowing ratio.

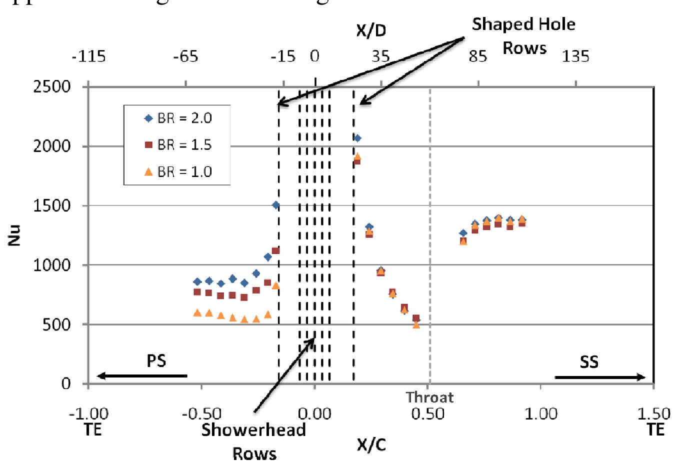

Figure 15: Effect of blowing ratio on Nusselt number distribution, M_{ex} = 0.85

For M_{ex} = 1.0 (Fig. 16), on the PS, the increase of blowing ratio did not raise the Nusselt number as much as it did for M_{ex} = 0.85 (Fig. 15); on the SS, the increase of blowing ratio even slightly reduced the Nusselt number. This trend may be caused by the reason discussed above in the section of Comparison with Showerhead-Only Vane. That is, the shaped hole cooling may reduce the surface heat flux in some cases. On one hand, for the M_{ex} = 1.0 case, because the boundary layer shear stress is so large, the disrupting effect of injection is not that remarkable as compared with the boundary layer turbulent fluctuation, so the increase of the blowing ratio changes the Nusselt number very little; on the other hand, the injection is adding kinetic energy into the boundary layer, and moderates the velocity gradient, therefore, reduces the turbulent shear stress in the boundary layer. The effect of injection flow reducing boundary layer turbulence will increase as the blowing ratio increases, thus for M_{ex} = 1.0, on SS, higher blowing ratios results in lower Nusselt numbers. Also at M_{ex} = 1.0, shock may occur on the SS surface, causing the effect of blowing ratio on the Nusselt number to behave differently from that at M_{ex} = 0.85 (Fig. 15). The exact reason of how transonic exit flow (M_{ex} = 1.0) influence the heat transfer behavior with shaped holes will be a subject for further research, perhaps including some CFD analysis.

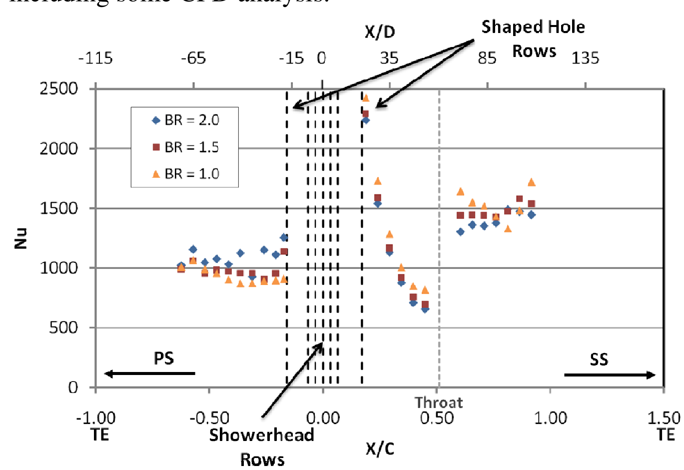

Figure 16 : Effect of blowing ratio on Nusselt number distribution, M_{ex} = 1.0

NHFR Comparison

Net heat flux reduction is a measure to evaluate the overall film cooling performance of coolant injection. Net heat flux reduction is defined below in equation 12.

$$NHFR = 1 - \frac{q''}{q_0''} = 1 - \frac{h}{h_0}\left(1 - \frac{\eta}{\phi}\right) \qquad (12)$$

In this equation ϕ refers to the overall film cooling effectiveness defined as in equation 13.

$$\phi = \frac{T_w - T_r}{T_c - T_r} \qquad (13)$$

This value is assumed to be between 0.5 and 0.7 according to Mehendale and Han[47]. A value in the middle of this range

(0.6) will be used for NHFR analysis. This value has been used by Mehendale and Han [47], Drost *et al.* [53], and Nasir *et al.* [34] for high speed cascade studies. Heat transfer coefficient is normalized by heat transfer coefficient data taken by Nasir *et al.* [34] on a solid, uncooled vane without cooling holes in the same facility. This method was also used by Mehendale and Han [47] to normalize heat transfer coefficient.

Figure 17 compares NHFR data recorded by Nasir *et al.* [34] on a showerhead-only film cooled vane using the same transient TFG technique as the present study. As was the case with film effectiveness, the showerhead and shaped hole film cooled vane shows higher film cooling performance across the entire measurement surface with NHFR values an average of 2.6x higher across the measurement surface. Similar Nusselt number values combined with film effectiveness values 2-2.5x that of Nasir *et al.* [34] result in very large NHFR increases on the PS. On the SS, lower heat transfer augmentation from shaped hole film cooling results in slightly smaller gains over the showerhead-only case. However, the comparison supports the findings of the film effectiveness comparison: that film cooling performance is greatly improved downstream of the leading edge by adding shaped holes on the PS and SS. Again, this average 2.6x NHFR increase occurs with only a 1.6x increase in the required coolant mass flow.

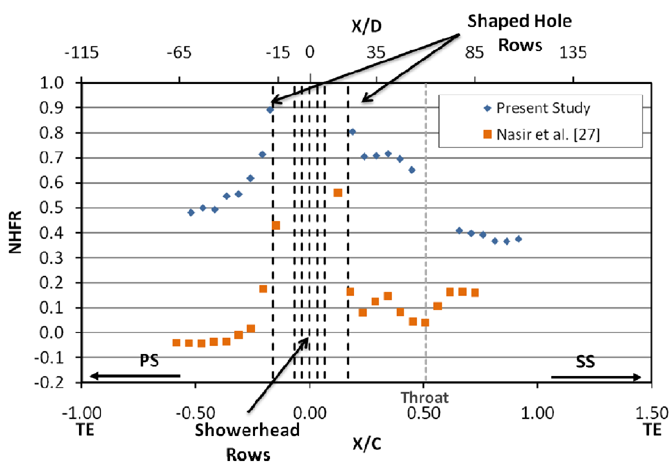

Figure 17: Comparison of NHFR from Nasir *et al.* [34] with the present study

CONCLUSIONS

Film cooling performance tests were conducted for three exit Mach number/Reynolds number combinations: 1.0/1,400,000; 0.85/1,150,000; and 0.60/850,000. At exit Mach numbers of 1.0 and 0.85 three blowing ratio conditions were tested: BR = 1.0, 1.5, and 2.0. All tests were performed at high freestream turbulence levels with inlet turbulence intensity of 12% and turbulence length scale normalized by the cascade pitch of 0.28. Vane surface film cooling effectiveness and net heat flux reduction distributions were presented and compared with literature. The chief conclusions of the study are as follows:

Film cooling effectiveness data compared well in both level and trend with existing shaped hole literature at similar conditions. Stanton number compared favorably with analytical laminar and turbulent flat plate boundary layer solutions, with expected trends reported on the PS and SS.

The addition of shaped hole rows downstream of showerhead injection on both the PS and SS of the vane resulted in film effectiveness levels averaging 2-2.5x those of a showerhead only film cooled vane. The addition of shaped holes was also shown to augment heat transfer considerably in the near hole region on the SS and PS.

A comparison of NHFR between a showerhead only and combined showerhead and shaped hole film cooled vane showed that the addition of a single row of shaped holes to both the PS and SS of the vane resulted in considerably increased NHFR (2.6x the value of showerhead-only NHFR) downstream of the holes. This analysis showed that the addition of shaped holes reduced the amount of heat absorbed by the PS and SS over showerhead-only injection, with only 1.6x increase in coolant mass flow required.

For constant Mach number, increasing blowing ratio showed increases in film effectiveness and heat transfer augmentation on the PS. Little significant increase in film effectiveness or heat transfer augmentation in SS data may due to the small change on SS shaped hole blowing ratio.

AKNOWLEDGEMENT

The authors are thankful to Solar Turbines for supporting this research and granting the permission to publish the results. Special thanks to Eli Razinsky for his encouragement. Dr. Richard Anthony (AFRL) provided the thin film gages used in this study, without his help this research will not be possible. The authors highly appreciate Dr. Ekkad's for his helpful discussions and Colin Reagle's for his assistance on the tests. The authors are also grateful to The Connecticut Center for Advanced Technology, Inc. for their help on the machining of the shaped holes.

NOMENCLATURE

h	heat transfer coefficient
k	thermal conductivity
M	Mach number
Re	Reynolds number
Nu	Nusselt number
PS	pressure surface
q''	heat flux
r	recovery factor
SS	suction surface
T	temperature
t	time
TFG	thin film gauge
Tu	streamwise freestream turbulence intensity

U	local velocity
x	vane surface distance from stagnation point
C	true chord
y	surface depth
D	cooling hole diameter
A	area
BR	blowing ratio
LE	leading edge
NHFR	net heat flux reduction
$\dot{m}$	mass flow rate
MFR	mass flow ratio

Greek

γ	ratio of specific heats
ρ	local density
η	adiabatic effectiveness
φ	overall film cooling effectiveness

Subscripts

∞	freestream
aw, w	adiabatic wall, wall
ex	exit
i	initial, inlet
o	uncooled
r	recovery
s	surface
c	coolant
x	vane surface distance from stagnation point

REFERENCES

[1] Goldstein, R. J., Lau, K. Y., and Leung, C. C., 1983, "Velocity and Turbulence Measurements in Combustion Systems," *Experiments in Fluids*, Vol. 1, pp. 93-99.

[2] Koutmos, P. and McGuirk, J. J., 1989, "Isothermal Flow in a Gas Turbine Combustor A Benchmark Experimental Study," *Experiment in Fluids*, Vol. 7, pp. 344-354.

[3] Reiss, H., Bölcs, A., 2000, "The Influence of the Boundary Layer State and Reynolds Number on Film Cooling and Heat Transfer on a Cooled Nozzle Guide Vane," *IGTI Turbo Expo,* Berlin, GT-2000-205.

[4] F. E. Ames, 1998, "Aspects of Vane Film Cooling With High Turbulence: Part I— Heat Transfer," *Journal of Turbomachinery*, 1998, Vol. 120 / 775.

[5] S.M. Guo, M.L.G. Oldfield, and A.J. Rawlinson, 2002, "Influence of Discrete Pin Shaped Surface Roughness (P-Pins) on Heat Transfer and Aerodyanmics of Film Cooled Aerofoil," *Proceedings of ASME Turbo Expo* GT-2002-30179.

[6] J. Michael Cutbirth and David G. Bogard, 2002, "Evaluation of Pressure Side Film Cooling With Flow and Thermal Field Measurement, Part II: Turbulence Effects," *Proceedings of ASME Turbo Expo* GT-2002-30175.

[7] Shichuan Ou, Richard Rivir, Matthew Meininger, Fred Soechting, and Martin Tabbita, 2000, "Transient Liquid Crystal Measurement of Leading Edge Film Cooling Effectiveness and Heat Transfer with High Free Stream Turbulence," *Proceedings of ASME Turbo Expo* GT-2000-245.

[8] Goldstein, R. J., Eckert, E. R. G., and Burggraf, F., 1974, "Effects of Hole Geometry and Density on Three-Dimensional Film Cooling," Int. *J. Heat Mass Transfer*, **17**, pp. 595–607.

[9] Schmidt, D., Sen, B., and Bogard, D., 1996, "Film Cooling with Compound Angle Holes: Adiabatic Effectiveness," *ASME J. Turbomachinery*, **118**, pp. 807-813

[10] Gritsch, M., Schulz, A., and Wittig, S., 1998, "Heat Transfer Coefficients Measurements of Film-Cooling Holes With Expanded Exits," *IGTI Conference*, Stockholm, Paper 98-GT-28.

[11] Y. Yu, C.H. Yen, T.I.P. Shih, M.K. Chyu and S. Gogineni, 2002, "Film cooling effectiveness and heat transfer coefficient distributions around diffusion shaped holes," *ASME J. Heat Transfer,* **124**, pp. 820–827.

[12] Bell, C. M., Hamakawa, H., Ligrani, P. M., 2000, "Film Cooling From Shaped Holes," *ASME J. Heat Transfer,* **122**, pp. 224–232.

[13] Dittmar, J., Schulz, A., Wittig, S., 2003, "Assessment of Various Film-Cooling Configurations Including Shaped and Compound Angle Holes Based on Large-Scale Experiments," *ASME J. Turbomachinery*, **125**, pp. 57-64

[14] Yuen, C. H. N., Martinez-Botas, R. F., and Whitelaw, J. H., 2001, "Film Cooling Effectiveness Downstream of Compound and Fan-Shaped Holes," *IGTI Turbo Expo*, New Orleans, Paper 2001-GT-0131.

[15] Lu, Y., Dhungel, A., Ekkad, S. V., Buker, R. S., 2009, "Effect of Trench Width and Depth on Film Cooling from Cylindrical Holes Embedded in Trenches," *ASME J. Turbomachinery*, **131**, pp. 1-13

[16] Dhungel, A., Lu, Y., Phillips, W., Ekkad, S. V., Heidmann, J., 2009, "Film Cooling From a Row of Holes Supplemented with Antivortex Holes," *ASME J. Turbomachinery*, **131**, pp. 1-13

[17] Wittig, S., Schulz, A., Gritsch, M., Thole, K. A., 1996, "Transonic Film-Cooling Investigations: Effects of Hole Shapes and Orientations," *IGTI Turbo Expo*, Birmingham, UK, Paper 1996-GT-222.

[18] Thole, K. A., Gritsch, M., Schulz, A., Wittig, S., 1998, "Flowfield Measurements for Film-Cooling Holes With Expanded Exits," *ASME J. Turbomachinery*, **120**, pp. 327-336

[19] Saumweber, C., Schulz, A., 2004, "Interaction of Film Cooling Rows: Effects of Hole Geometry and Row Spacing on the Cooling Performance Downstream of the Second Row of Holes," *ASME J. Turbomachinery*, **126**, pp. 237-246

[20] Saumweber, C., and Schulz, A., 2003, "Interaction of Film Cooling Rows: Effects of Hole Geometry and Row Spacing on the Cooling Performance Downstream of the Second Row of Holes," *IGTI Turbo Expo*, Atlanta, Paper GT2003-38195.

[21] Colban, W., Gratton, A., Thole, K. A., Haendler, M., 2005, "Heat Transfer and Film-Cooling Measurements on a Stator Vane with Fan-Shaped Cooling Holes," *IGTI Turbo Expo*, Reno-Tahoe, Paper GT2005-68258.

[22] Colban, W., Thole, K. A., Haendler, M., 2007, "Experimental and Computational Comparisons of Fan-Shaped Film Cooling on a Turbine Vane Surface," *ASME J. Turbomachinery*, **129**, pp. 23-31

[23] Chappell, J., Ligrani, P., Sreekanth, S., Lucas, T., 2008, "Suction-Side Gill-Region Film Cooling: Effects of Hole Shape and Orientation on Adiabatic Effectiveness and Heat Transfer Coefficient," *IGTI Turbo Expo*, Berlin, Paper GT2008-50798.

[24] Furukawa, T., Ligrani, P., 2002, "Transonic Film Cooling Effectiveness from Shaped Holes on a Simulated Turbine Airfoil," *AIAA J. Thermophysics and Heat Transfer,* **16**, pp. 228-237

[25] Zhang, L., Pudupatty, R., 2000, "The Effects of Injection Angle and Hole Exit Shape on Turbine Nozzle Pressure Side Film-Cooling," *IGTI Turbo Expo,* Munich, Paper 2000-GT-247.

[26] Zhang, L., Moon, H. K., 2008, "The Effect of Wall Thickness on Nozzle Suction Side Film Cooling," *IGTI Turbo Expo,* Berlin, Paper GT2008-50631.

[27] Schnieder, M., Parneix, S., von Wolfersdorf, J., 2003, "Effect of Showerhead Injection on Superposition of Multi-Row Pressure Side Film Cooling with Fan Shaped Holes," *IGTI Turbo Expo,* Atlanta, Paper GT2003-38693.

[28] Thurman, D. R., Poinsatte, P. E., Heidmann, J. D., 2008, "Heat Transfer Measurements for a Film Cooled Turbine Vane Cascade," *IGTI Turbo Expo,* Berlin, Paper GT2008-50651

[29] Guo, S. M., Lai, C. C., Jones, T. V., Oldfield, M. L. G., Lock, G. D., Rawlinson, A. J., 1998, "The application of thin-film technology to measure turbine-vane heat transfer and effectiveness in a film-cooled, engine-simulated environment," *Int. J. Heat and Fluid Flow,* **19**, pp. 594-600

[30] Sargison, J. E., Guo, S. M., Oldfield, M. L. G., Lock, G.. D., Rawlinson, A. J., 2002, "A Converging Slot-Hole Film-Cooling Geometry—Part 2: Transonic Nozzle Guide Vane Heat Transfer and Loss," *ASME J. Turbomachinery,* **124**, pp. 461-471

[31] Reagle, C. J., Newman, A., Xue, S., Ng, W., Ekkad, S., Moon, H. K., Zhang, L., 2010, "A Transient Infrared Technique for Measuring Surface and Endwall heat Transfer in a Transonic Turbine Cascade," *IGTI Turbo Expo,* Glasgow, Paper GT2010-22975

[32] Bolchoz, T., Nasir, S., Reagle, C., Ng, W.F., and Moon, H.K., 2009, "An Experimental Investigation of Showerhead Film Cooling Performance In A Transonic Vane Cascade At Low and High Freestream Turbulence," *IGTI Turbo Expo,* Orlando, Paper GT2009-59796.

[33] Nasir, S., Carullo, J.S., Ng, W.F., Thole, K.A., Wu, H., Zhang, L.J., and Moon, H.K., 2007, "Effects of Large Scale High Freestream Turbulence, and Exit Reynolds Number on Turbine Vane Heat Transfer in a Transonic Cascade," *ASME J. Turbomachinery*, **131**, pp.021021-1 to -11.

[34] Nasir,S., Bolchoz, T., Ng, W.F., Zhang, L.J., Moon, H.K., Anthony, R.J., 2008, "Showerhead Film Cooling Performance of a Turbine Vane in a Transonic Cascade," *ASME IMECE 2008,* Paper 66528.

[35] C. Camci, 1989, "an Experimental and Numerical Investigation of Near Cooling Hole Heat Fluxes on a Film-Cooled Turbine Blade," *ASME J. Turbomachinery*, **111**, pp. 63-70.

[36] Doorly, J.E., Oldfield, M.L.G., 1987, "The Theory of Advanced Multi-Layer Thin Film Heat Transfer Gages," *Int. J. Heat and Mass Transfer*, **30**, pp. 1159–1168.

[37] Joe, C.R., 1997, "Unsteady Heat Transfer on the Turbine Research Facility at Wright Laboratory," Ph.D. Dissertation, Syracuse University.

[38] Cress, R.D., 2006, "Turbine Blade Heat Transfer Measurements in a Transonic Flow Using Thin film Gages," Master's Thesis, Virginia Polytechnic Institute and State University.

[39] Popp, O., Smith, D.E., Bubb, J.V., Grabowski, H.C., Diller, T.E. Schetz, J.A., Ng. W.F., 2000, "An Investigation of Heat Transfer in a Film Cooled Transonic Turbine Cascade, Part II: Unsteady Heat Transfer," *IGTI Turbo Expo,* Berlin, Paper GT-2000-203.

[40] Ekkad, S. V., Han, J. C., Du, H., 1998, "Detailed Film Cooling Measurements on a Cylindrical Leading Edge Model: Effect of Free-Stream Turbulence and Coolant Density," *ASME J. Turbomachinery,***120,** pp. 799-807.

[41] Moffat, R. J., 1988, "Describing Uncertainties in Experimental Results," *Exp. Thermal and Fluid Science*, **1**, pp. 3-17.

[42] Brown, K.H., Coleman, H.W., and Steele, W.G., 1995, "Estimating Uncertainty Intervals for Linear Regression," AIAA-1995-0796.

[43] Andrew, Newman, 2010, "Performance of a Showerhead and Shaped Hole Film Cooled Vane at High Freestream Turbulence and Transonic Conditions," Master's Thesis, Virginia Polytechnic Institute and State University.

[44] Incropera, F.P. and DeWitt, D.P., 2002, Fundamentals of Heat and Mass Transfer, 5th Ed., John Wiley and Sons, New York.

[45] Blair, M. F., 1983, "Influence of Free-Stream Turbulence on Turbulent Boundary Layer Heat Transfer and Mean Profile Development, Part I—Experimental Data," *ASME J. Heat Transfer,* **105,** pp. 33-40.

[46] Gillis, J. C., and Jhonston, J. P., 1983, "Turbulent Boundary Layer Flow and Structure on a Convex Wall and its Redevelopment on a Flat Wall," Journal of Fluid Mechanics, Vol. 135, pp. 123-153.

[47] Mehendale, A.B., Han, J.-C., 1993, "Reynolds number Effect on Leading Edge Film Effectiveness and Heat Transfer Coefficient," *Int. J. Heat and Mass Transfer*, **36**, pp. 3723–3730.

[48] E. Lutum, J. von Wolfersdorf, K. Semmler, S. Naik, B. Weigand, 2001, "Film Cooling on a Convex Surface: Influence of External Pressure Gradient and Mach Number on Film Cooling Performance," *Heat and Mass Transfer*, **38**, 7-6.

[49] Shantanu Mhetras, Je-Chin Han, and Ron Rudolph 2008, "Film-Cooling Effectiveness From Shaped Film Cooling Holes for a Gas Turbine Blade," *Proceedings of ASME TURBO EXPO* 2008 Power for Land, Sea and Air, GT-2008-50916

[50] Abuaf, N., Bunker, R., Lee, C. P., 1997, "Heat Transfer and Film Cooling Effectiveness in a Linear Airfoil Cascade," *ASME J. Turbomachinery,***119,** pp. 302-309

[51] Arts, T., Bourguignon, A.E., 1990, "Behavior of a Coolant Film with Two rows of Holes along the Pressure Side of a High Pressure Nozzle Guide Vane," *ASME J. Turbomachinery*, **112**, pp. 512-520.

[52] Ekkad, S.V., Mehendale, A.B., Han, J.-C., Lee, C.P., 1997, "Combined Effect of Grid Turbulence and Unsteady Wake on Film Effectiveness and Heat Transfer Coefficient of a Gas

Turbine Blade with Air and CO2 Film Injection," *ASME J. Turbomachinery*, **119**, pp. 594-600.
[53] Drost, U., Bölcs, A., 1999, "Investigation of Detailed Film Cooling Effectiveness and Heat Transfer Distribution on a Gas Turbine Airfoil," *ASME J. Turbomachinery*, **121,** pp. 233-242.